

# Development of Aluminum Nitride Single-Crystal Substrates

Issei SATOH\*, Satoshi ARAKAWA, Keisuke TANIZAKI, Michimasa MIYANAGA, Takashi SAKURADA, Yoshiyuki YAMAMOTO and Hideaki NAKAHATA

Sublimation growth of aluminum nitride (AlN) single crystals was investigated. The crystals were prepared by two methods: By slicing *c*-plane-grown thick crystals along the *m*-plane and by heteroepitaxial growth on *m*-plane SiC substrates. Defects of the crystals were observed by a high-resolution transmission electron microscope. The dislocation density in AlN/SiC (0001) decreased significantly at about 1.5  $\mu\text{m}$  above the interface, while stacking faults were initiated from the interface toward the growth surface in AlN/SiC (1-100). With increasing crystal thickness, the dislocation density decreased up to  $5 \times 10^4/\text{cm}^2$  at a thickness of 10 mm. In an AlN single crystal grown on SiC (0001), the dislocations were localized around the AlN/SiC interface, and far fewer dislocations occurred near the growth surface. Thick, highly crystalline AlN single crystals could be grown on SiC (0001) substrates.

Keywords: AlN, single crystal, substrate, nonpolar, sublimation

## 1. Introduction

High-frequency, high-power semiconductor devices are widely used in electric vehicles, medical equipment, home appliances, and communication equipment. Recently, there has been a growing demand for semiconductors that have such characteristics as high withstand voltage, high speed and high-temperature operation, low power consumption and radiation resistance.

To meet this demand, silicon carbide (SiC) is increasingly being used as a substrate material instead of silicon (Si), which is reaching the limit of its material properties. For the next generation, the substrate material needs to possess a higher breakdown field and to operate under higher frequencies (Fig. 1). Meanwhile, mercury lamps have been used as ultraviolet (UV) light sources for cleaning applications in semiconductor processing and sterilization in the medical field. It would be advantageous to be able to produce a stable, high-output UV light by a small device that requires no mercury and can start instantly;

these characteristics can be realized by the use of UV light-emitting diodes (LEDs). To date, UV-LEDs have been fabricated on sapphire and various other substrate materials. This has resulted in disorder in the crystalline structure inside the emitting layer (crystal defects) and also led to a low luminous efficiency because of the differences between the lattice constant and the crystal structure.

Aluminum nitride (AlN) is a promising candidate for UV applications and high-power devices because of the following advantages: The widest bandgap (6.2 eV) in direct-transition semiconductors, a high thermal conductivity of 3.3 W/cmK, and excellent electrical insulation properties. High-quality single-crystal substrates are in demand for use in high-efficiency and high-power devices. AlN, particularly a bulk AlN single crystal, is a promising substrate material for these devices because of the small differences in lattice constants and thermal expansion coefficients between AlN and  $\text{Al}_{1-x}\text{Ga}_x\text{N}$  ( $0 \leq x \leq 1$ ) epitaxial layers.

Bulk AlN single crystals are commonly grown from the vapor phase, e.g., by sublimation<sup>(1)</sup> or by the hydride vapor-phase epitaxial (HVPE) method,<sup>(2)</sup> because their high melting point makes it difficult to grow them from the melt phase. During sublimation, the raw material is sublimated at a high temperature and then its vapor is recondensed in a lower-temperature area. Thus far two techniques have been reported to grow bulk AlN single crystals without AlN seeds: spontaneous nucleation without a seed crystal<sup>(3)</sup> and heteroepitaxial growth using a foreign substrate such as SiC<sup>(4),(5)</sup>. The former can produce high-quality crystals, but has difficulties with both the growth of larger crystals and reproducibility. The latter can produce large crystals with relative ease; however, the quality of the crystals is not as high as with the former method because of lattice mismatch and SiC decomposition at high temperatures. We have already succeeded in growing free-standing AlN single crystals with high crystalline quality by using *c*-plane SiC as seed substrates<sup>(6)-(9)</sup>.

Figure 2 shows the structure and surface orientation of an AlN crystal. As the effect of a piezoelectric field can be suppressed, field-effect transistors (FETs) and other

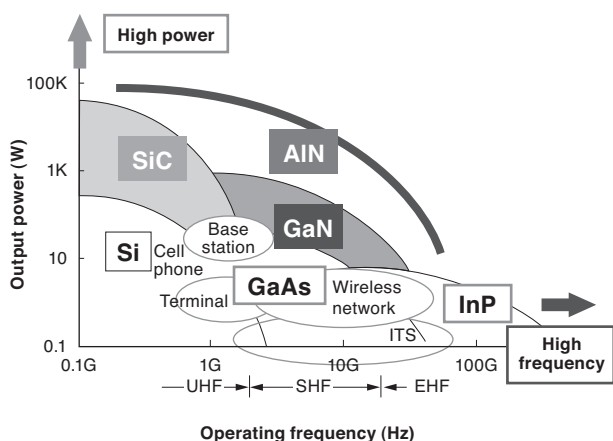


Fig. 1. Frequency ranges and output power of electronic devices using various semiconductors.

electronic devices on nonpolar planes, such as the *m*-plane, can be expected to operate in a normally-off mode and thus save power. Furthermore, it has been suggested that by fabricating UV-LEDs on the nonpolar planes, we can obtain high efficiency characteristics<sup>(10),(11)</sup>. This has been achieved on nonpolar SiC substrates by the same research group. The dislocation density of an AlN epilayer grown on a *c*-plane SiC substrate was  $3 \times 10^8$  /cm<sup>2</sup>, while that of an AlN grown on an *m*-plane SiC substrate was  $4 \times 10^9$  /cm<sup>2</sup>. Although the dislocation density of an *m*-plane SiC substrate is higher by one order of magnitude, the emission intensity from a device on this substrate has been reported to be about 25 times greater than that on a *c*-plane substrate<sup>(12)</sup>. Using nonpolar planes in AlN substrate materials instead of the SiC substrate is expected to improve the quality of epilayer and device characteristics; however, there exists very few reports on nonpolar bulk AlN single crystals<sup>(13),(14)</sup>. In one study, a dislocation density of  $2.9 \times 10^5$  /cm<sup>2</sup> was observed for *m*-plane AlN substrates cut from crystals of size  $11 \times 13$  mm<sup>2</sup> grown along the *c*-axis<sup>(13)</sup>.

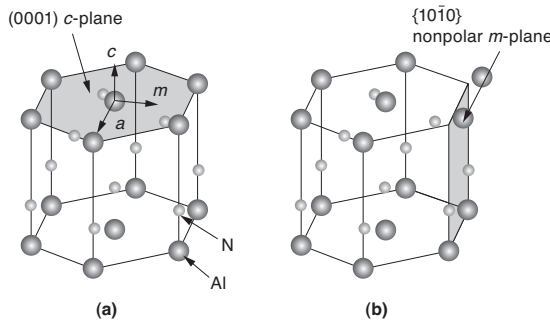


Fig. 2. Crystal structure and orientation of AlN.

There are two methods for preparing nonpolar-oriented bulk substrates: i) By slicing *c*-plane-grown thick crystals along the *m*-plane and ii) by heteroepitaxial growth on *m*-plane SiC substrates (Fig. 3). However, there has been no report comparing the merits of these methods. This review reports on the *c*-plane and *m*-plane growth of bulk AlN single crystals, the defect characterization of these crystals, surface polishing of single-crystal AlN substrates, and the achievement of highly crystalline, nonpolar single-crystal AlN substrates.

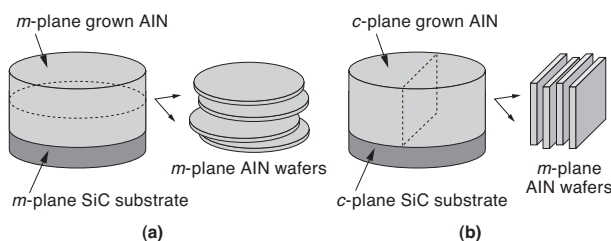


Fig. 3. Preparation methods for nonpolar AlN single-crystal substrates.

## 2. Experimental

Bulk AlN single crystals were grown by sublimation on 4H-SiC (0001)<sub>Si</sub> and (1-100) substrates. An AlN powder source was placed in a high-density graphite-based crucible and heated by radio-frequency induction. The source was held at high temperatures of 1900–2250°C, and the SiC substrates were placed in an area where the temperature was lower than that of the raw material ( $\Delta T = 100$ –500°C). N<sub>2</sub> gas was introduced into the furnace during the crystal growth and was maintained at a reduced pressure of 10–100 kPa. The resulting sample was sliced and polished in order to investigate the dislocation behavior of AlN grown on SiC. To evaluate the crystal quality of the AlN, X-ray diffraction (XRD) measurements were conducted. AlN crystals were etched in a molten KOH + NaOH mixture to bring the etch pits into existence. To estimate the etch pit density (EPD), the etched surfaces were observed under a Nomarski microscope. To investigate the dislocation behavior in more detail, the cross sections and plan views of the AlN single crystals were observed using a high-resolution transmission electron microscope (HR-TEM).

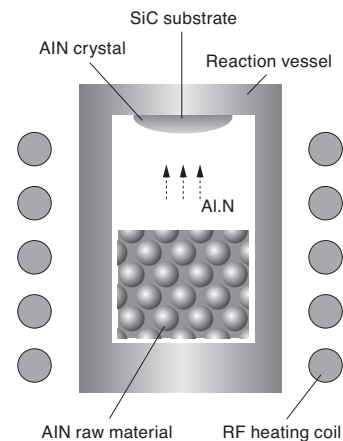
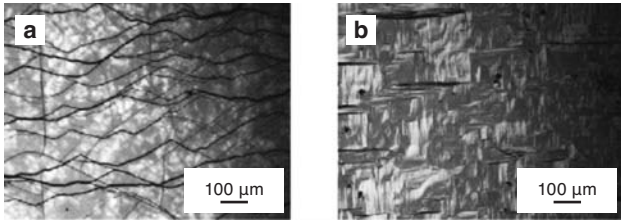


Fig. 4. Schematic diagram of sublimation method.

## 3. Surface Morphology of AlN Single Crystals

AlN single crystals were grown on *c*-plane (4° off) and *m*-plane SiC substrates by sublimation. We observed the growth surfaces using a Nomarski microscope. On the *c*-plane the surface morphology reflecting the corresponding step off, which indicates the part of the hexagonal structure, was observed (Fig. 5). In addition, surface morphology, such as 4-symmetry, was observed on the *m*-plane by x-ray diffraction; nonpolar (10-10) of AlN was found that the grown crystal was a single crystal (Fig. 6). An X-ray rocking curve (XRC) of the FWHM of the *c*-plane AlN grown on SiC (0002) and that of the *m*-plane AlN grown on SiC (10-10) were 47 and 1500 arcsec, respectively. Thus, AlN grown on *m*-plane SiC has poor crystalline quality compared to AlN grown on *c*-plane SiC.



**Fig. 5.** Nomarski microscope images of an AlN crystal surface: (a) *c*-plane AlN sample grown on *c*-plane SiC, and (b) *m*-plane AlN sample grown on *m*-plane SiC.

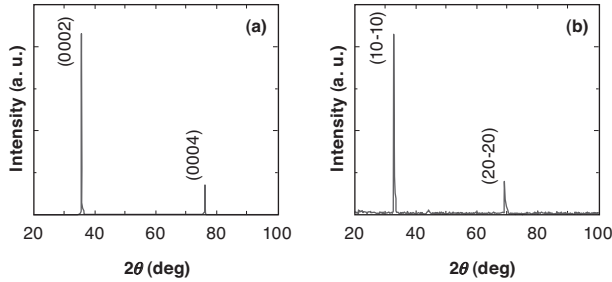


**Fig. 6.** XRD  $2\theta$ - $\omega$  patterns: (a) *c*-plane AlN sample grown on *c*-plane SiC, and (b) *m*-plane AlN sample grown on *m*-plane SiC.

#### 4. Defect Characterization of AlN Single Crystals Grown on *c*-plane and *m*-plane SiC

**Figures 7** and **8** show cross-sectional and plan-view TEM images of AlN grown on (a) SiC (0001) and (b) SiC (1-100). For the *m*-plane growth, the defects of AlN were observed in both directions, as shown in **Figs. 7 (b)** and **8 (b)**; this indicates that most of the defects are plane faults. Most defects stretch from the AlN/SiC interface to the growth surface. The fringes appeared when the incident beam was inclined  $1^\circ$  to the sample surface, which indicates that these defects are stacking faults (**Fig. 7 (c)**). Most of the stacking faults seem to start at the AlN/SiC interface and point toward the growth surface in the AlN/SiC (1-100) sample (**Fig. 7 (b)**). To reduce these faults, it might be necessary to introduce a buffer layer at the initial growth stage.

On the other hand, the dislocation density in *c*-plane growth decreased significantly at about  $1.5 \mu\text{m}$  above the interface. The dislocations are expected to move easily and to localize around the interface because the AlN crystal growth by sublimation was performed at high temperatures. It is assumed that the interface dislocations can release the lattice mismatch strain around the interface and yield high quality crystals. This result matches with the XRD data described in the previous section. Thick AlN single crystals of high crystalline quality could be grown on SiC (0001) substrates.

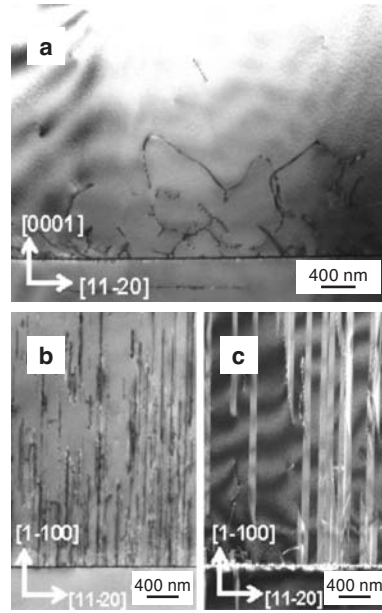


**Fig. 7.** Cross-sectional TEM images (bright field) of (a) AlN/SiC (0001) and (b) AlN/SiC (1-100). (c) (dark field) fringes appearing when the incident beam was inclined  $1^\circ$  to the sample surface.

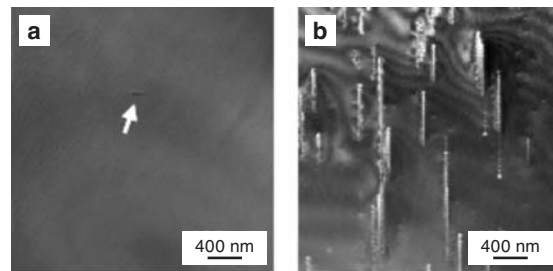


**Fig. 8.** Plan-view TEM images (bright field) of AlN at a distance of  $30 \mu\text{m}$  from the AlN/SiC interface: (a) *c*-plane AlN sample grown on *c*-plane SiC, and (b) *m*-plane AlN sample grown on *m*-plane SiC.

#### 5. Dislocation Behavior and Estimation of Etch Pit Density after Polishing

To obtain low-defect AlN substrates, thick crystals were grown. To observe the dislocations in the middle of the growth, it is necessary to remove the damaged layers that are introduced during the slicing of the crystals. **Figure 9** shows the Nomarski microscope images of the different polished surfaces after KOH + NaOH etching. The etch pits can be clearly seen on the surface prepared by chemical mechanical polishing (CMP), while the surface prepared by mechanical polishing (MP) has a damaged layer so that the surface is etched overall (**Fig. 9**). The dislocation density obtained by counting etch pits is of the same order as the density obtained from the plan-view TEM observations, and the value which is reported by the other groups in the thickness range of up to  $2 \text{ mm}^{(11),(12)}$ .

**Figure 10** shows that with increasing crystal thickness, the dislocation density decreases up to  $5 \times 10^4 / \text{cm}^2$  at a thickness of 10 mm<sup>(16),(17)</sup>. We note that in the AlN single crystal grown on SiC (0001), the dislocations were localized around the AlN/SiC interface, and far fewer dislocations occurred near the growth surface<sup>(15)</sup>. The values reported by other groups<sup>(18),(19)</sup> are also shown in **Fig. 10**. A few groups have reported a value as low as  $1.2 \times 10^4 / \text{cm}^2$ , but there was no information about the distance from the interface<sup>(13),(19)</sup>.

Compared to the reported values of the dislocation density of AlN epitaxial layers grown on sapphire and SiC, which are  $10^8$ – $10^9 / \text{cm}^2$ , the AlN crystals obtained in this study are clearly of sufficiently high quality.

*c*- and *m*-plane AlN substrates were cut from the crystals and the surfaces were polished. Atomic Force Microscope (AFM) images of the substrates are shown in **Fig. 11**. The surface roughness (root mean square; RMS) was 0.2 nm or less for both planes, and thus confirms that the polishing levels can be used for epitaxial growth.

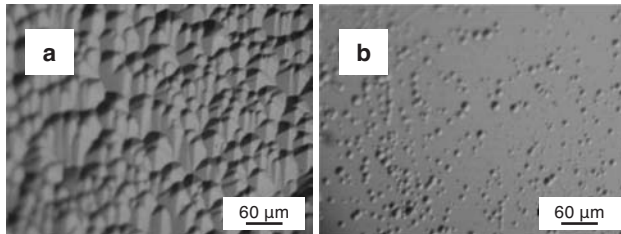


**Fig. 9.** Nomarski microscope images after etching the surface with molten KOH-NaOH: (a) Mechanical polishing, (b) chemical mechanical polishing.

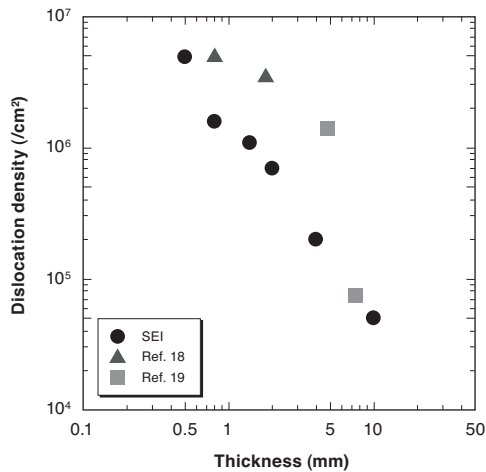


**Fig. 10.** AlN crystal thickness dependence of the dislocation densities estimated by counting etch pits.

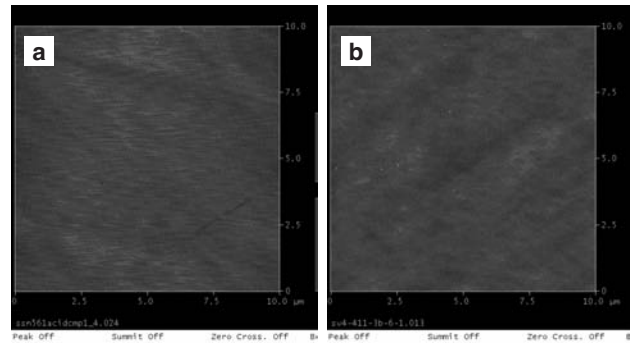


**Fig. 11.** AFM images of AlN surface after polishing: (a) *c*-plane AlN (RMS, 0.20 nm), (b) *m*-plane AlN (RMS, 0.15 nm).

## 6. Conclusion

We summarize the results of our study as follows:

- i. The dislocation density of AlN/SiC (0001) decreased significantly at about 1.5 μm above the interface, while stacking faults stretched from the interface toward the growth surface in AlN/SiC (1-100).
- ii. With increasing crystal thickness, the dislocation density decreased up to  $5 \times 10^4 / \text{cm}^2$  at a thickness of 10 mm. Thick AlN single crystals of high crystalline quality could be grown on SiC (0001) substrates.
- iii. By polishing the *m*-plane AlN substrate cut from the *c*-plane grown AlN crystal, a surface RMS of 0.2 nm was achieved, indicating that this approach is suitable for producing substrate for epitaxial growth.

This study was partly supported by the New Energy and Industrial Technology Development Organization (NEDO), “Development of Nitride-based Semiconductor Single Crystal Substrate and Epitaxial Growth Technology.”

**Figures 6, 7, 9, and 10** are reprinted with permission from Ref. (17).

## References

- (1) G. A. Slack and T. F. McNelly, *J. Crystal Growth* 34, 263 (1976).
- (2) Y. Melnik *et al.*, *Phys. Stat. Sol.* 200 (1) 22 (2003).
- (3) B. M. Epelbaum, M. Bickermann, and A. Winnacker, *J. Crystal Growth* 275, 479 (2005).
- (4) E. N. Mokhov *et al.*, *J. Crystal Growth* 281, 93 (2005).
- (5) Y. Shi *et al.*, *MRS Internet, J. Nitride Semicond. Res.* 6, 5 (2001).
- (6) M. Tanaka, S. Nakahata, K. Sogabe, H. Nakahata, and M. Tobioka, *Jpn. J. Appl. Phys.* 36, L1062 (1997).
- (7) M. Miyanaga *et al.*, *SEI Technical Review* 63, 22 (2006).
- (8) M. Miyanaga, N. Mizuhara, S. Fujiwara, M. Shimazu, H. Nakahata, and T. Kawase, *J. Crystal Growth* 300, 45 (2007).
- (9) N. Mizuhara, M. Miyanaga, S. Fujiwara, H. Nakahata, and T. Kawase, *Phys. Stat. Sol. C* 4, 2244 (2007).
- (10) Y. Taniyasu, M. Kasu, and T. Makimoto, *Nature* 441, 325 (2006).
- (11) Y. Taniyasu *et al.*, *Appl. Phys. Lett.* 90, 261911 (2007).
- (12) Y. Taniyasu *et al.*, 55th JSAP Spring Meeting, 29p-B-9 (2008) [in Japanese].
- (13) R. T. Bondokov *et al.*, *J. Crystal Growth* 310, 4020 (2008).
- (14) A. Sedhain *et al.*, *Appl. Phys. Lett.* 95, 262104 (2009).

- (15) S. K. Mathis *et al.*, J. Crystal Growth 231, 371 (2001).  
(16) I. Satoh *et al.*, 56th JSAP Spring Meeting, 1a-ZJ-1 (2009) [in Japanese].  
(17) I. Satoh, S. Arakawa, K. Tanizaki, M. Miyanaga, and Y. Yamamoto, Phys. Stat. Sol. C 7, 1767 (2010).  
(18) P. Lu *et al.*, J. Crystal Growth 310, 2464 (2008).  
(19) T. Kato *et al.*, Proceedings of ICNS-8, MP49 (2009).

**Contributors** (The lead author is indicated by an asterisk (\*)).

**I. SATOH\***

- Ph. D.

Assistant Manager, Semiconductor Materials R&D Department, Semiconductor Technologies R&D Laboratories

He is engaged in the research and development of nitride semiconductor substrates.



**S. ARAKAWA**

- Semiconductor Materials R&D Department, Semiconductor Technologies R&D Laboratories

**K. TANIZAKI**

- Ph. D.

Semiconductor Materials R&D Department, Semiconductor Technologies R&D Laboratories

**M. MIYANAGA**

- Assistant General Manager, Electronics & Materials R&D Laboratories

**T. SAKURADA**

- Assistant General Manager, Semiconductor Materials R&D Department, Semiconductor Technologies R&D Laboratories

**Y. YAMAMOTO**

- Manager, Semiconductor Materials R&D Department, Semiconductor Technologies R&D Laboratories

**H. NAKAHATA**

- Ph. D.

General Manager, Semiconductor Materials R&D Department, Semiconductor Technologies R&D Laboratories